

Supporting Information

Microfluidic system for in-flow reversible photoswitching of near-infrared fluorescent proteins

Vladislav V. Lychagov^{1,2}, Anton A. Shemetov^{1,2}, Ralph Jimenez^{3,4,*} and Vladislav V. Verkhusha^{1,2,5,*}

¹Department of Anatomy and Structural Biology and ²Gruss-Lipper Biophotonics Center, Albert Einstein College of Medicine, Bronx, New York 10461, USA

³JILA, National Institute of Standards and Technology and ⁴Department of Chemistry and Biochemistry, University of Colorado, Boulder, Colorado 80309, USA

⁵Department of Biochemistry and Developmental Biology, Faculty of Medicine, University of Helsinki, Helsinki 00029, Finland

Abstract

Here we present additional information on optical scheme functioning, formation of multiple beam structured illumination pattern, energy of excitation/switching irradiation used in experiments and principal scheme of the experimental setup. Next, we describe some additional results for single-point experiment, calibration procedure and in-flow switching experiment.

Details on experimental system

Design of optical system.

We used laser diode (LD) modules from Power Technology IQu2A100 and IQu2A105 emitting at 643 nm and 783 nm, respectively. To produce evenly spaced multiple beams of equal intensities, two identical diffractive optical elements (DOEs; HOLOEYE) were used (Figure 2A). Each element split the incident laser beam into 5×5 beams pattern with 0.1° at 640 nm (0.12° at 780 nm) angular distance between beams, along with suppression of higher orders of diffraction. Lenses L1, $f_1=125$ mm and L2, $f_2=150$ mm were used to handle these beams and to make the first intermediate diffraction patterns in the joint focal planes of lenses L1-L3 and L2-L3 ($f_3=20$ mm), where the spatial filters SF 783 nm and SF 643 nm were installed (Figure 2B). These filters were necessary to remove unwanted beams from the first intermediate diffraction patterns and to form the second, total intermediate diffraction pattern in the joint focal plane of lenses L4, $f_4=50$ mm. Dichroic mirror DM1 (Chroma T6851pxr) and lenses L4 were used to combine intermediate diffraction patterns from the 643 nm and the 783 nm lasers and to pass them with the help of the objective lens L5, $f_5=10$ mm into the object plane inside the microfluidic channels MFC. Additional beam stopper could be installed between lenses L4 to selectively remove any of five cycles of switching in the final beams pattern. Dichroic mirror DM2 (Chroma T660lpxr) reflects laser light toward the microfluidic chip MFC and transmits collected fluorescent signal toward the PMT (Hamamatsu R10699), and a light-emitting diode (LED) light toward the image sensor Cam. Dichroic mirror DM3 (Chroma 89016bs) separates fluorescence from LED light.

Electronics and detection.

Fluorescence photons collected by the optical system is detected by a PMT operated at -600 – 700 V. Current output of the PMT loads input of a custom-built transimpedance amplifier with a gain of 300 V/A, and output voltage of the amplifier is digitized by the data acquisition (DAQ) board NI PCIe-6351. This DAQ board has analog outputs used for controlling laser diodes. Data acquisition and processing software along with utilities for controlling peripheral devices connected to PC were realized in the NI LabVIEW programming environment (Figure S1).

Table S1. Energy in J/cm², which a droplet receives in a single beam.

Wavelength, nm		643 nm				783 nm	
Exposure time, ms	Flow speed, mm/s	Irradiance, W/cm ²		Irradiance, W/cm ²		Irradiance, W/cm ²	
		176.84	84.00	44.21	23.87	129.98	63.66
3.64	11	0.64	0.31	0.16	0.09	0.47	0.23
2.67	15	0.47	0.22	0.12	0.06	0.35	0.17
1.60	25	0.28	0.13	0.07	0.04	0.21	0.10

The intensity row contains values of average intensity in a single beam and the speed column specifies droplet speeds for which stable droplet generation and flow was possible. Exposure time was estimated from the beam diameter and droplet speed, and exposure energy was calculated as a product of fluence and exposure time.

643 nm laser diode intensity – 80 mW. 643 nm intensity on the sample with DOE installed, 25 beams – 55.5 mW. 643 nm intensity on the sample with DOE installed, 1 beam – 2.22 mW. 783 nm laser diode intensity – 90 mW. 783 nm intensity on the sample with DOE installed, 25 beams – 41 mW. 783 nm intensity on the sample with DOE installed, 1 beam – 1.63 mW. All measurements were made by Coherent LabMax-TO with VIS head.

Figure S1. Principal scheme of the experimental setup and the interconnections between the key components.

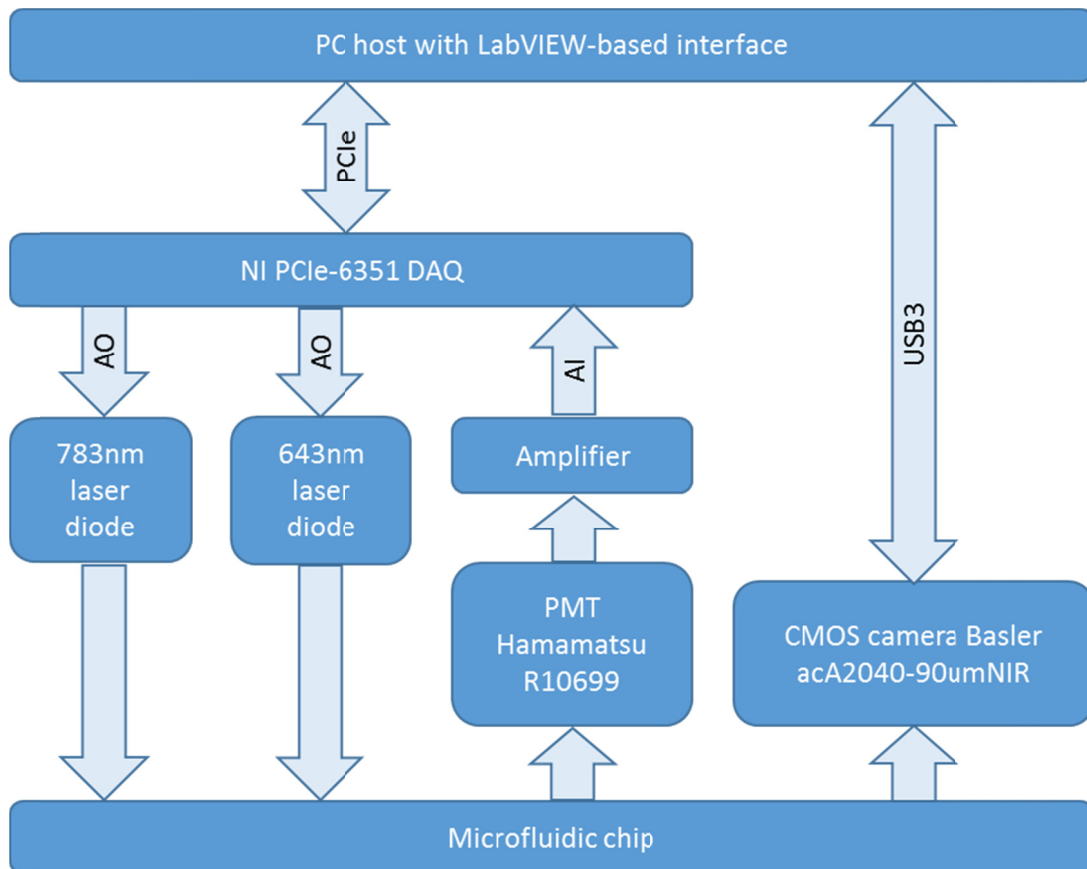
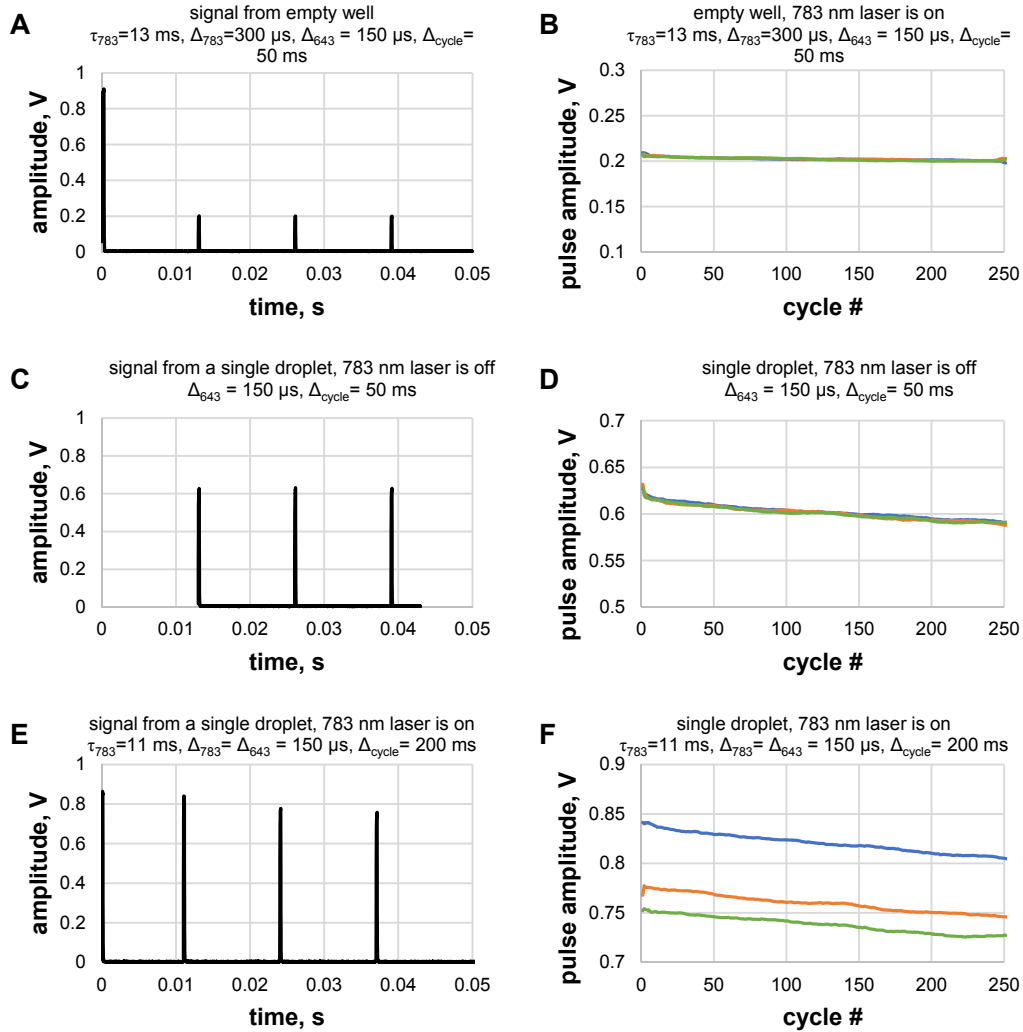
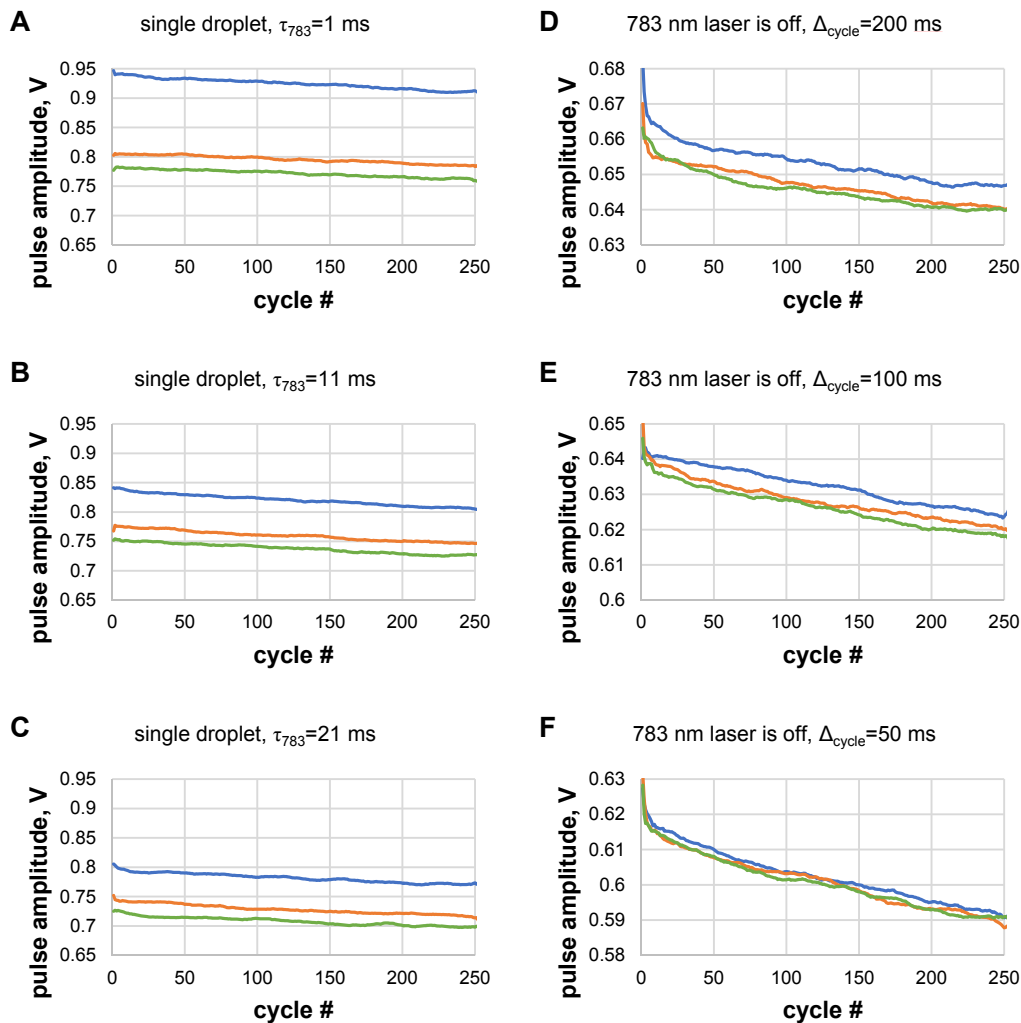


Figure S2. Examples of the raw pulsed signals (single photoswitching cycle) and changes in the signal amplitude with the number of photoswitching cycle. 783 nm pulse irradiance was 4 kW/cm² and 643 nm laser pulses were 1.2 kW/cm².



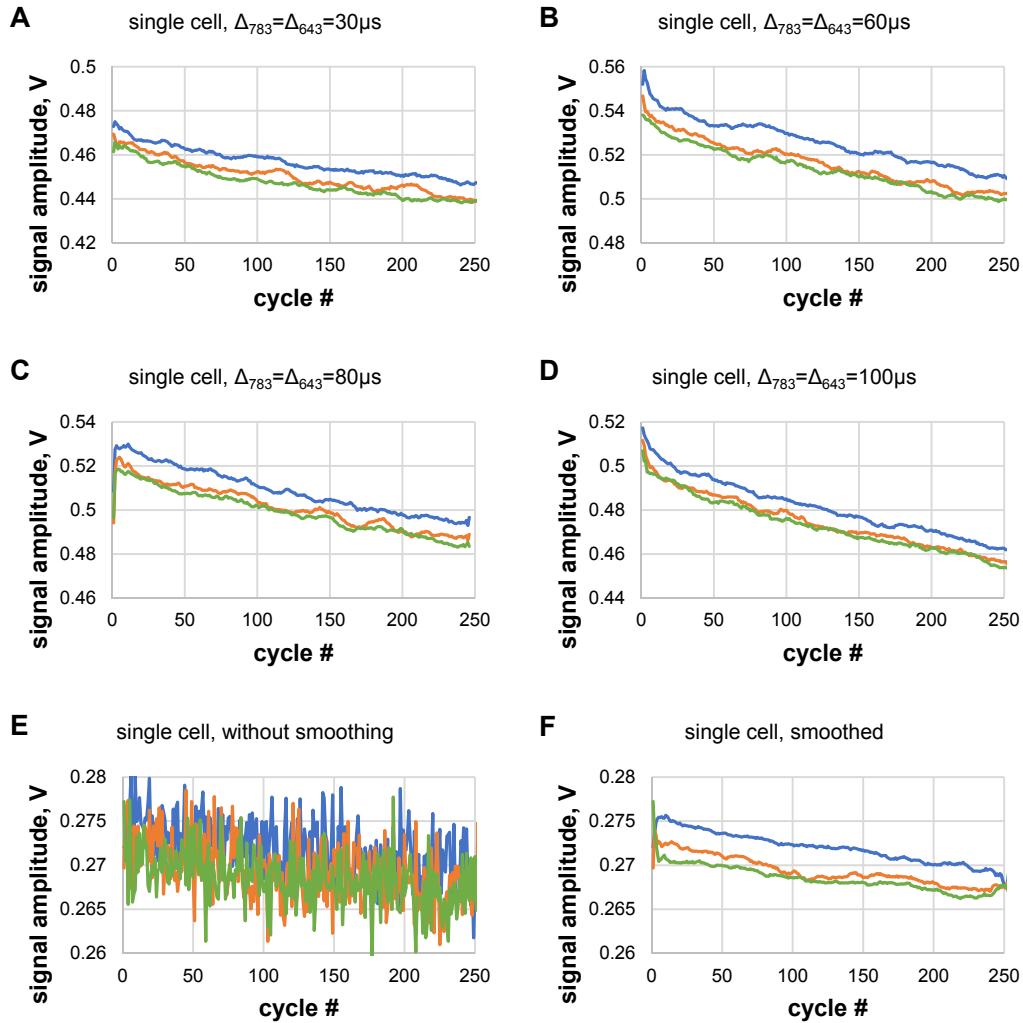
Raw pulsed signals (A, C, E) detected in single-point measurements and dependence of amplitude of the pulses on the number of switching cycle (B, D, F). (A, B) Signal from an empty well indicates background level. (C, D) Signal from a single droplet shows absence of switching, when the 783 nm laser is off. (E, F) Difference in amplitudes of the pulses indicates switching, when the 783 nm laser is on.

Figure S3. Dependence of photoswitching contrast on parameters of excitation/photoswitching laser pulses in experiment with a single droplet. 783 nm pulse irradiance was 4 kW/cm² and 643 nm laser pulses were 1.2 kW/cm².



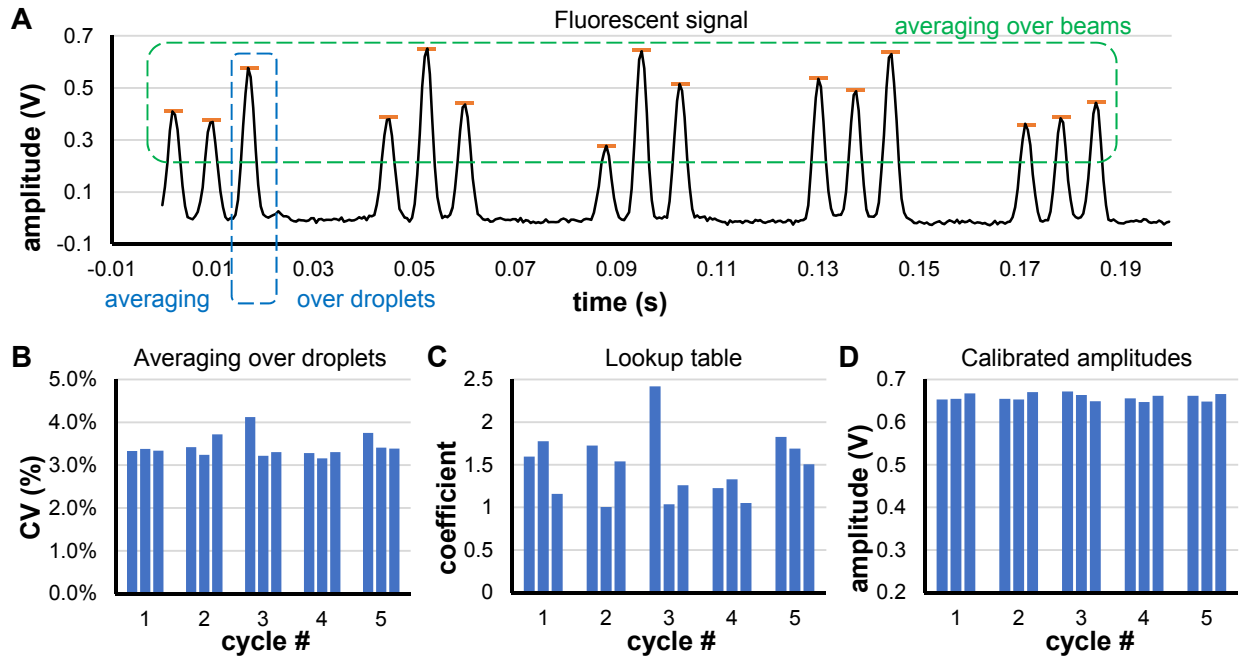
(A-C) Dependence of switching contrast on time delay τ_{NIR} between the 783 nm laser pulse and the 643 nm laser pulses: $\Delta_{783}=\Delta_{643}=150$ μs , $\Delta_{\text{cycle}}=200$ ms. (D-F) Dependence of uncontrollable transition of the protein into Pr form on the dwell-time between consecutive cycles: $\Delta_{643}=150$ μs .

Figure S4. Dependence of photoswitching contrast on parameters of excitation/photoswitching laser pulses in experiment with a single cell. 783 nm pulse irradiance was 4 kW/cm^2 and 643 nm laser pulses were 1.2 kW/cm^2 .



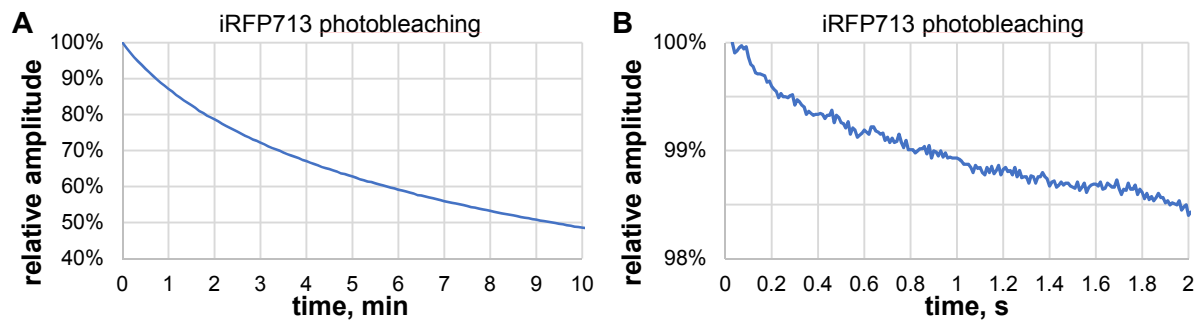
(A-D) Dependence of switching contrast on the energy of switching/excitation pulse: $\tau_{783}=1 \text{ ms}$, $\Delta_{\text{cycle}}=50 \text{ ms}$. Amount of energy depends on the pulse width Δ_{783} and Δ_{643} , while intensity is constant. Slow decrease in intensity indicates photobleaching, which is more expressed for higher energies/longer pulses, while switching contrast remains constant within 250 cycles. (E-F) Filtering of initial data recovered from the pulsed signal allows to observe switching in a cell.

Figure S5. In-flow measurements of constitutively fluorescent iRFP713 protein.



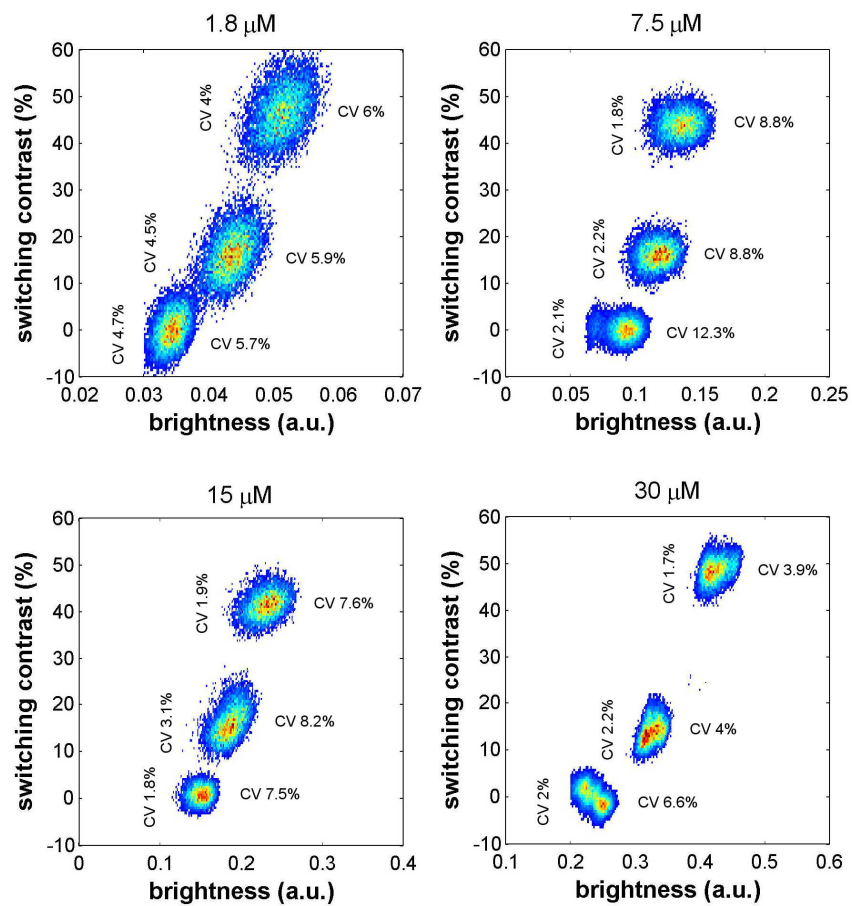
(A) Fluorescent signal (solid black line) and amplitudes of fluorescent pulses (red ticks) detected by processing software. (B) Droplet-to-droplet variation of amplitude for every pulse in the signal. (C) Array of calibration coefficients calculated using iRFP713. (D) Array of amplitudes of the fluorescent signal after calibration.

Figure S6. Photobleaching of constitutively fluorescent iRFP713 protein.



(A) Long-term and (B) short-term photobleaching of the purified iRFP713 solution are shown.

Figure S7. Dependence of switching contrast on brightness of droplets with different concentrations of DrBphP-PCM purified protein.



DrBphP-PCM protein concentrations (1.8 – 30 μM) are indicated at the top of the panels. The coefficients of variation (CVs) for the protein switching contrast and for the protein brightness are indicated at the left and right sides of the respective dotplots.